IMAGING METHODOLOGY – Notes

Magnetic Resonance in Medicine 80:272–278 (2018)

Demonstration of Velocity Selective Myocardial Arterial Spin Labeling Perfusion Imaging in Humans

Terrence R. Jao[1]* and Krishna S. Nayak[2]

Purpose: Transit delay is a potential source of error in cardiac arterial spin-labeled (ASL) in heart failure or with collateral circulation. This study demonstrates the feasibility of using transit delay insensitive velocity selective ASL and compares its performance with flow-sensitive alternating inversion recovery (FAIR) ASL.

Methods: Velocity selective labeling was achieved using an adiabatic BIR8 preparation. FAIR and velocity-selective ASL (VSASL) with various velocity cutoffs ($V_C = 10$–40 cm/s) and labeling directions (anterior–posterior X, lateral–septal Y, and apical–basal Z) were carried out in 10 healthy volunteers (1F/9M age 23–30 y). Myocardial blood flow (MBF) and temporal signal-to-noise (TSNR) were measured.

Results: VSASL sensitivity to perfusion decreased with increasing V_C. At low V_C (<5 cm/s), spurious labeling of myocardium occurs and overestimates MBF. MBF measured with FAIR (1.12 ± 0.26 ml/g/min) and VASL (1.26 ± 0.27 ml/g/min) at V_C of 10 cm/s in Z were comparable (TOST with difference of 0.30 ml/g/min, $P = 0.049$). TSNR was 2.8 times larger using FAIR (13.62 ± 5.25) than in VSASL (4.87 ± 1.58). VSASL was insensitive to perfusion in the Y direction. X and Z performed similarly with TSNR of 4.17 ± 2.32 and 3.97 ± 0.56, respectively.

Conclusion: VSASL is a promising alternative to FAIR ASL in the heart and is well suited for scenarios when transit delays are long. **Magn Reson Med 80:272–278, 2018. © 2017 International Society for Magnetic Resonance in Medicine.**

Key words: myocardial perfusion imaging; arterial spin labeling; cardiovascular magnetic resonance; transit delay; myocardial blood flow; velocity selective labeling

INTRODUCTION

Arterial spin-labeled (ASL) cardiac magnetic resonance (CMR) is a promising non-contrast technique for mapping myocardial blood flow (MBF). Other modalities such as single-photon emission computed tomography (SPECT), positron emission tomography (PET), or first-pass perfusion CMR rely on intravenous contrast agents and/or are unsuitable for patients with poor renal clearance or who require frequent evaluations. ASL avoids these drawbacks by using magnetic preparations to label the blood itself as a source of endogenous contrast. In the heart, flow-sensitive alternating inversion recovery (FAIR) has been the most commonly used labeling scheme, whereby a slab-selective inversion containing the imaging slice is used for control preparations and a non-selective inversion is used for labeled preparations (1–3).

For single-slice acquisitions, FAIR has been demonstrated to obtain measurements of MBF that are comparable to those found using PET (4) and could detect clinically relevant changes in perfusion under vasodilation (5). However, in a multi-slice acquisition scheme, the FAIR inversion slab thickness must be increased to encompass the larger imaging volume. Zun et al. (3) found substantial underestimation of MBF at a mid-short axis slice by 68% when the FAIR inversion slab was increased from 3 to 12 cm. This suggests that FAIR is incompatible with multi-slice acquisitions because the thick inversion slab increases the spatial gap between the labeled edge and the imaging slices, leading to longer arterial transit times (ATT). Similarly, disease processes with slow coronary flows, such as heart failure (6,7) or circuitous coronary collateral vascularization, also exhibit prolonged ATT. Muehling et al. (8) found that the ATT because of collateral circulation (1.7 s) was significantly longer than antegradely perfused vessels (0.9 s) and vessels in healthy subjects (0.8 s). When ATT becomes much longer than the post-labeling delay, loss of ASL signal occurs and MBF is underestimated (9).

Velocity-selective ASL (VSASL) was developed in the brain to mitigate ASL signal loss caused by slow flow and long ATT (10). Blood is labeled based on its velocity by saturating spins above a velocity cutoff, termed V_C. In principle, VSASL can generate labels adjacent to tissue by choosing a low V_C to eliminate transit delay effects. In practice, choosing a high V_C along with a short inflow delay, TI, has the potential to generate large intravascular signals that could confound ASL measurements (11). In subtractive magnetic resonance angiography (MRA), this is seen as an advantage and VS pulses have recently been used to great effect in visualizing vasculature in both abdomen (12) and brain (13). In ASL, V_C, TI, and the velocity encoding direction must be considered more carefully to avoid intravascular signal. In brain, a V_C of 2 cm/s is used to match mean velocity within the small feeding arterioles while optimal TI was determined to be the T_1 of blood, which is ~1664 ms (11). Because of the tortuous path of small arterioles, Wong et al. (10) found that encoding direction had a negligible impact on perfusion measurements.

[1]Department of Biomedical Engineering, University of Southern California, Los Angeles, California, USA.

[2]Ming Hsieh Department of Electrical Engineering, University of Southern California, Los Angeles, California, USA.

Grant sponsor: National Institutes of Health; Grant number: R01-HL130494; Grant sponsor: American Heart Association; Grant number: 13GRNT13850012; Grant sponsor: Wallace H. Coulter Foundation.

*Correspondence to: Terrence Jao, 3740 McClintock Ave, EEB 400, University of Southern California, Los Angeles, CA 90089-2564. E-mail: tjao@usc.edu

Received 12 April 2017; revised 19 September 2017; accepted 13 October 2017

DOI 10.1002/mrm.26994

Published online 6 November 2017 in Wiley Online Library (wileyonlinelibrary.com).

The choice of V_C, TI, and encoding direction must be reevaluated in the heart because of the unique challenge of cardiac motion. Myocardium can move as fast as 2 cm/s (14,15) during stable diastole. Therefore, targeting blood within small arterioles may cause spurious labeling of the heart. A larger V_C must be used, which would label blood in the coronary tree. Coronary blood flow is pulsatile, with maximal velocities of >15–40 cm/s during diastole and almost no flow during systole. Coronary velocity also varies depending on disease states. Anderson et al. (16) found that peak coronary velocity was inversely proportional to the lumen area to left ventricular mass ratio; stenotic vessels had faster peak velocities. However, under hyperemia, this trend was reversed, possibly because of coronary steal. In the setting of hypertension, mean coronary velocity can reach upward of 51 cm/s, but when presented alongside left ventricular dysfunction, coronary velocities were similar to those in healthy vessels (~30 cm/s) (17).

In this work, we describe a practical implementation of cardiac VSASL and demonstrate its ability to measure myocardial perfusion in comparison to FAIR ASL. In humans, we experimentally determine the sensitivity of cardiac VSASL to selection of V_C and encoding direction.

METHODS

Velocity Selective Pulse

An adiabatic symmetric BIR-8 pulse described by Guo et al. (18,19) was used for VS labeling. Bloch simulation was used to simulate and optimize pulse parameters for a peak B_1 of at least 0.08 G and off-resonance range of ± 250 Hz, which is consistent with what can be reasonably expected in the heart at 3T (20,21). RF subpulses were 2.24 ms each with the following parameters, $\kappa = 62.96$, $\omega_{max} = 21.6$, and $\zeta = 20.5$. Single gradient lobes between RF sub pulses were replaced with bipolar gradients to avoid striping artifacts from occurring over myocardium, as described by Fan et al. (22). An additional delay of 0.5 ms after each bipolar gradient module was used to further reduce eddy current sensitivity. Bipolar gradients were designed to saturate spins above a designated velocity cutoff, V_C, for labeled acquisitions and were turned off during control acquisitions to impart similar T_2-weighting only. V_c is given by $V_c = \pi/(2\gamma M_1)$, where γ is the gyromagnetic ratio and M_1 is the first moment of the BIR8 gradient waveform with $M_1 = g(2T^2 + 6RT + 4R^2$, where g is the gradient amplitude, T is the duration of the plateau of an individual gradient lobe, and R is the ramp duration, which we set to 0.5 ms. The velocity selective BIR8 pulse encodes velocity into the phase of the MR signal. After tipping the transverse magnetization back into the longitudinal direction and spoiling, this produces a modulation in the longitudinal magnetization given by $M_z = M_0\cos(\beta v)$ where $\beta = \gamma M_1$, M_1 is first moment of the bipolar gradient waveforms, and v is velocity. Under assumptions of laminar flow, where the velocity distribution is uniform from 0 to twice the mean velocity, v_0, the velocity profile becomes sinc-shaped and is given by $M_z = M_0$ sinc($2\beta v$) (10). The cutoff velocity is defined as the first zero crossing of the sinc velocity profile and is given by $V_c = \pi/(2\beta)$.

The choice of pulse parameters was the result of significant experimental fine tuning in a spherical phantom. The settings described above are the results that produced the most consistent labeling with the fewest artifacts and shortest pulse duration.

Pulse performance was validated within the lumen of the right coronary artery (RCA) in 2 healthy volunteers. VS labeling with both the control (gradients off) and labeled (gradients on) settings was carried out immediately before imaging using centric view ordered GRE (FA = 5^0, pulse repetition time (TR) = 3.2, 64 × 64 matrix). An additional image without the VS preparation pulse was also acquired to measure saturation efficiency.

VSASL Acquisition

Cardiac VSASL was performed at a single mid-short axis slice illustrated in Figure 1, using cardiac-gated velocity selective (VS) labeling and balanced steady state free precession imaging. VS labeling was performed during mid-diastole, as determined from a cinema/video (CINE) scout scan. Imaging was performed during mid-diastole in the subsequent RR such that MBF estimates reflect the time-average perfusion rate of pulsatile blood flow over the course of one heartbeat. Background suppression using a single non-selective hyperbolic secant inversion pulse placed between labeling and imaging was designed to null myocardial T_1s between ~1250 ms and 1450 ms. The timing of the background suppression pulse was optimized for different heart rates and took into account T_2 signal loss from the VS labeling pulse (23). Image acquisition parameters were: TR/echo time (TE) of 3.2/1.5 ms, prescribed flip angle of 50, acquired matrix size of 96 × 96, GRAPPA (24 ACS, 60 acquired). FAIR ASL was performed using a similar pulse sequence without background suppression and used a 3-cm slice-selective and a non-selective hyperbolic secant inversion pulse for control and labeled acquisitions, respectively.

Six pairs of control and labeled images were acquired for MBF quantification. Each image pair was acquired with breath holding (10–12 s) to prevent misregistration and to avoid spurious VS labeling from respiratory motion. A 6-s delay between image acquisition allowed full recovery of the VS label. Control and labeled image acquisition order was alternated after each pair to avoid bias from the acquired order. A baseline image and a noise image were also acquired in an additional 2-s breath hold to calculate coil sensitivity maps and noise covariance matrix.

All images were acquired on a 3T GE Signa Excite HD using an 8-channel cardiac receiver array. Ten healthy volunteers were recruited for this study (1F/9M age 23–30 y). In 5 healthy volunteers, VSASL was carried out with 4 different V_c of 10, 20, 30, and 40 cm/s in the longitudinal (Z) encoding direction. In 1 volunteer, VSASL was performed at V_C of 5 cm/s and 15 cm/s. In 4 healthy volunteers, VSASL was performed using the radial (X, Y) and longitudinal (Z) encoding directions at V_C of 10 cm/s. Cardiac ASL using FAIR was acquired in each subject for comparison. The imaging protocol was approved by our institutional review board, and all subjects provided written informed consent.

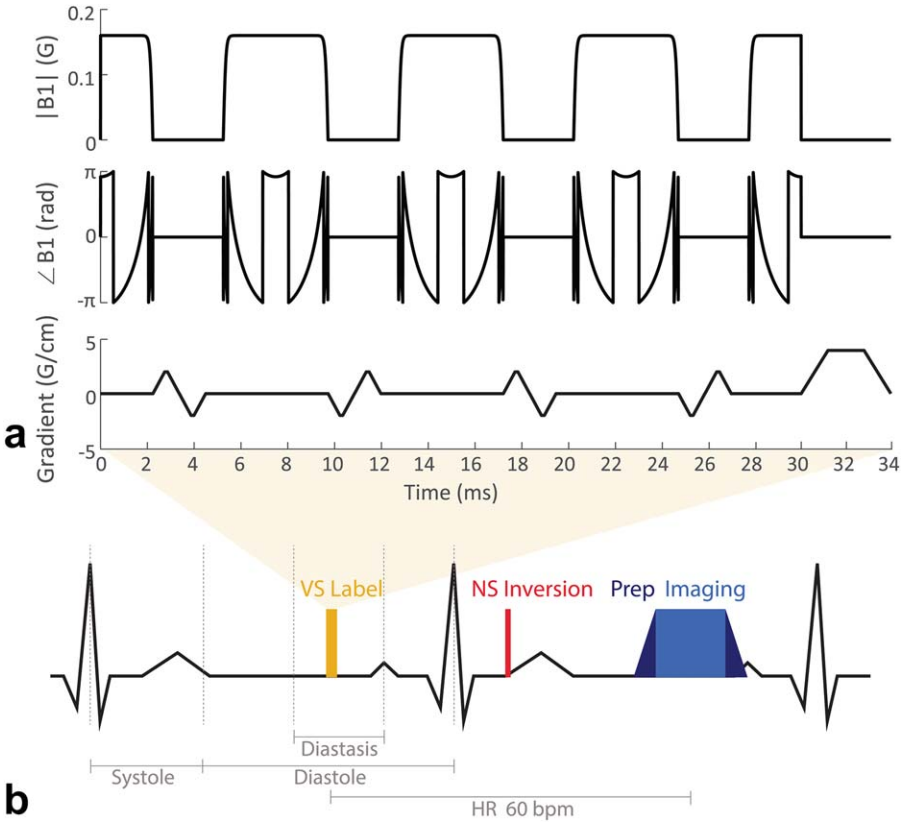

FIG. 1. VSASL pulse sequence. (**a**) The BIR8 pulse used for VS labeling. (**b**) The timing diagram of VSASL is to scale for a heart rate of 60 bpm. VS-labeling (orange) was performed during diastasis, when myocardial velocities are low and coronary flows are high. Imaging (blue) occurs 1 RR interval later. A single NS inversion (red) is placed between labeling and imaging for background suppression of myocardial T_1 of 1250–1450 ms.

Data Analysis

Images were reconstructed using GRAPPA and coil combined using optimal B_1 coil combination (24). The left ventricular (LV) myocardium was manually segmented in a single control and labeled image pair and the resultant masks were propagated through their respective image series using automatic motion correction (25). LV myocardium was divided into 6 segments in accordance with the AHA 17-segment standard (26) through a spatial averaging algorithm (27) to increase SNR for MBF estimation. MBF quantification was derived from Buxton's general kinetic model (28) at a single TI and was calculated using the following equation:

$$\mathrm{MBF} = \frac{\mathrm{L} - \mathrm{C}}{\alpha \times \mathrm{B} \times \mathrm{TI} \quad e^{-\frac{T_{VS}}{T_{2blood}}} \times e^{-\frac{TI}{T_{1blood}}}}. \qquad [1]$$

C, L, and B refer to the myocardial signal intensity within the control, labeled, and baseline image. α is the efficiency of the background suppression inversion pulse, whereas TI is the time between labeling and imaging, which is fixed according to the heart rate. We use the myocardial signal at baseline, B, rather than the fully relaxed magnetization of arterial blood, M_{0blood}, in Buxton's kinetic model for quantification. This is because, with the specific imaging parameters we use for snapshot SSFP, the myocardial signal provides a good approximation of M_{0blood} with almost no contrast between the 2. Two examples of these baseline images can be seen in Supporting Figure S1. An additional exponential term reflects T_2 signal loss from the VS pulse with duration T_{VS} in the transverse plane. T_{2blood} changes with hematocrit and oxygenation. Assuming an average hematocrit of 44% among subjects and 100% oxygenation saturation in healthy volunteers, T_{2blood} was found to be 120 ms (29). With T_{VS} of 25.5 ms and a T_{2blood} of 120 ms, this corresponds to a 19% signal loss. Physiological noise (PN) was calculated in the same way as Zun et al. (3) with the following equation:

$$\mathrm{PN} = \sqrt{\frac{\sigma^2_{odd} + \sigma^2_{even}}{2N_{pair}}}. \qquad [2]$$

σ^2_{odd} and σ^2_{even} correspond to variance of MBF in odd and even breath holds. Temporal SNR (TSNR) is a metric for the consistency of the MBF measurements in an individual and was calculated as the ratio of MBF to PN

$$\mathrm{TSNR} = \frac{\mathrm{MBF}}{\mathrm{PN}}. \qquad [3]$$

RESULTS

Validation of VS Labeling in RCA

Figure 2 shows the performance of the VS pulse within the RCA in 2 healthy volunteers. In the control setting (left image), coronary blood within the RCA was preserved, whereas in the labeled setting (right image), blood within the RCA was saturated. Saturation efficiency within the coronary lumen was measured at 89.7% and 74.6% for each volunteer, respectively.

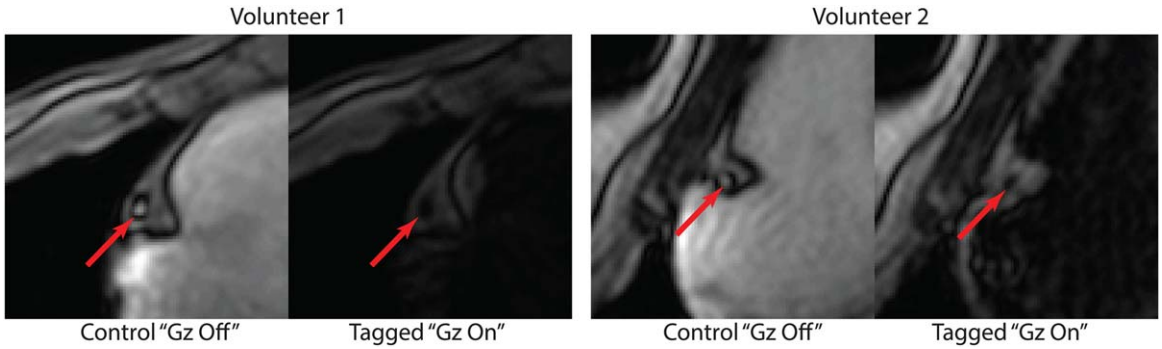

FIG. 2. Demonstration of VS labeling within the RCA of 2 healthy volunteers. Red arrows indicate location of RCA. Control acquisitions have gradients turned off, labeled acquisitions have gradients turned on. V_C was set at 10 cm/s. Saturation efficiency within the coronary lumen was 89.7% and 74.6% for volunteers 1 and 2, respectively. Images were not acquired with breath-holding. In volunteer 1, spurious tagging of the chest wall is likely because of respiratory motion.

Sensitivity to Velocity Cutoff

Figure 3 contains MBF (left) and TSNR (right) for FAIR and VSASL at cutoffs of 10, 20, 30, and 40 cm/s for septal, lateral, and all segments averaged across 5 subjects. Error bars for MBF are in dotted black and represent the average physiological noise across subjects to reflect measurement variability. Error bars for TSNR are in solid black and were calculated as the standard deviation of the TSNR between subjects to reflect intersubject variability. TSNR in individual subjects can be found in Supporting Table S1. Septal and lateral segments are defined in the illustration of the heart; septal segments correspond to anteroseptal and posteroseptal segments of the AHA 17-segment model (26) whereas lateral segments correspond to the anterolateral and posterolateral segments. Global MBF for VSASL (1.26 ± 0.27 ml/g/min) at V_C of 10 cm/s was similar to MBF for FAIR (1.12 ± 0.09 ml/g/min), but had lower TSNR of 4.87 ± 1.58 and 13.62 ± 5.25, respectively. These measurements of MBF are comparable to literature values using PET, which are 0.95 ± 0.28 ml/g/min (30) and 0.985 ± 0.230 ml/g/min (31), and first-pass CMR perfusion, which are 1.02 ± 0.22 ml/g/min (32). A two one-sided test (TOST) (33) at a difference of 0.3 ml/g/min showed that MBF was statistically equivalent with a *P*-value of 0.049 while a paired t-test showed that TSNR was statistically different with a *P*-value of 0.005. As V_C increased, both estimated MBF and TSNR decreased. MBF and TSNR were consistently lower in lateral segments compared with septal segments. A paired t-test showed statistical difference with *P*-values of 0.035 and 0.005, respectively. Figure 4 shows representative MBF maps for a single volunteer using FAIR and VSASL at V_C of 5 cm/s and 15 cm/s. MBF of septal segments were 1.09, 1.70, and 1.62 ml/g/min whereas MBF for lateral segments were 1.12, 5.64, and 1.34 ml/g/min for FAIR and VSASL at V_C of 5 cm/s and 15 cm/s, respectively.

Sensitivity to Encoding Direction

Figure 5 shows MBF (left) and TSNR (right) for FAIR and VSASL at the apical–basal (Z), anterior–posterior (X), and lateral–septal (Y) encoding directions averaged across 4 subjects. MBF and TSNR in individual subjects can be found in Supporting Table S2. X and Y encoding directions are defined in the illustration of the heart in Figure 5a. Lateral–septal Y severely underestimated MBF (0.41 ± 0.34 ml/g/min) and had the lowest TSNR (1.26 ± 1.03) when compared to FAIR ASL, which had a MBF of 1.27 ± 0.14 ml/g/min and TSNR of 10.26 ± 4.17. Anterior–posterior X underestimated MBF (0.95 ± 0.31 ml/g/min) to a lesser extent whereas apical–basal Z slightly overestimated MBF (1.74 ± 0.46 ml/g/min). TSNR was approximately equal between X (4.18 ± 2.32) and Z (3.98 ± 0.56), but X had more intersubject variability. Septal and lateral segments were not found to have statistically different MBF and TSNR.

DISCUSSION

This study demonstrates the feasibility of myocardial VSASL with background suppression. VSASL was able to yield a measurable signal difference within human myocardium and obtain MBF estimates similar to those reported in FAIR ASL (1,4,5,34–36).

This study also investigated how V_C and encoding direction affected the VSASL signal globally as well as in septal and lateral segments individually. When V_C increased, labeling efficiency and VSASL signal decreased, which lead to an underestimation of MBF. There was also a statistical difference between MBF and TSNR found in septal and lateral segments with changing V_C. Lateral segments consistently underestimated MBF and had lower TSNR than septal segments at $V > 10$ cm/s. This could be because of poorer labeling efficiency of the left circumflex artery that supplies the region. In contrast, at low $V_C \leq 5$ cm/s, lateral segments overestimated MBF. We suspect that this is because of spurious labeling of moving myocardium in the lateral wall that was not resolved with background suppression (15).

As opposed to VSASL in brain (10), we found that myocardial VSASL was sensitive to encoding direction. MBF and TSNR had the lowest intersubject variation in the longitudinal Z direction. Surprisingly, anterior–posterior (X) and lateral–septal (Y) directions performed very differently; X achieved similar MBF and TSNR as Z whereas Y severely underestimated MBF. This may be because of the coronary geometry, with no major vessels

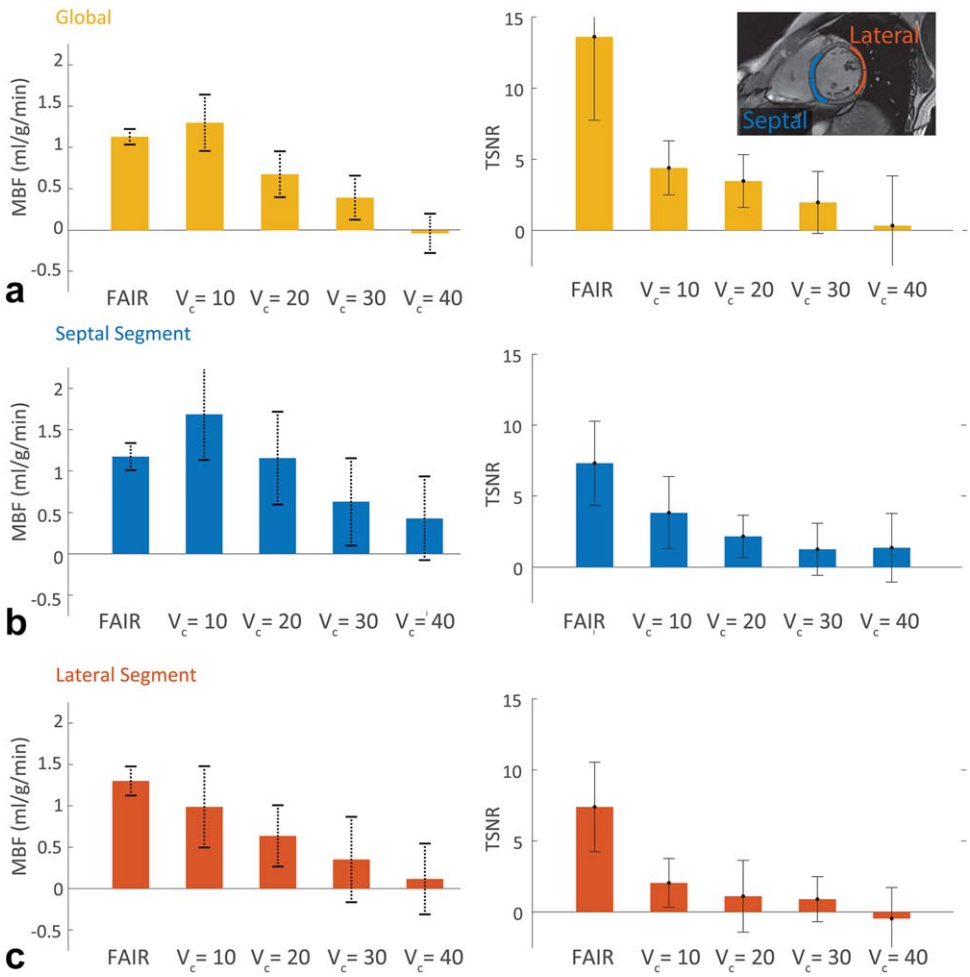

FIG. 3. VSASL sensitivity to V_C. (**a**) MBF and TSNR measured globally (yellow) decreases when V_C increases because of poor labeling efficiency. VSASL at V_C of 10 cm/s has statistically equivalent MBF as FAIR using the TOST procedure at a difference of 0.3 ml/g/min ($P = 0.049$). TSNR in VSASL at all cutoffs was consistently lower than in FAIR ($P \leq 0.005$). The inset displays the location of septal (blue) and lateral (red) segments used in regional analysis follows the AHA 17-segment model for the mid short axis slice. (**b**) MBF and TSNR in the septum. (**c**) MBF and TSNR in the lateral wall. We suspect that off-resonance in the lateral wall causes greater degradation of pulse performance. This lead to greater underestimation of MBF and lower TSNR in lateral segments when compared to the septum ($P = 0.035$ and $P = 0.005$, respectively). Error bars for MBF are in dotted black and represent the average physiological noise across subjects to reflect measurement variability. Error bars for TSNR are in solid black and were calculated as the standard deviation of the TSNR between subjects to reflect intersubject variability.

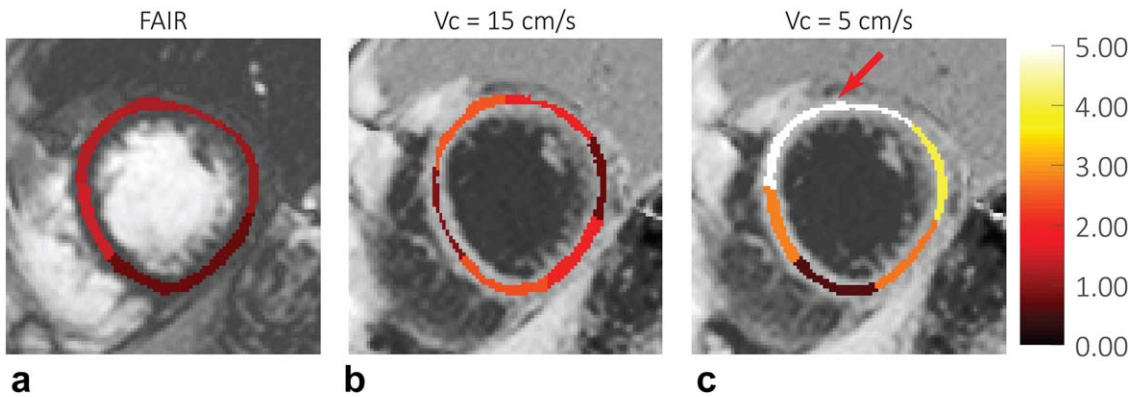

FIG. 4. Representative MBF map in a single volunteer. (**a**) The FAIR MBF map is displayed over the control image. FAIR has spatially homogenous MBF. (**b**) The VSASL MBF map at V_C of 15 cm is comparable to the MBF map in FAIR. Contrast of the VSASL control image is inverted because of the single inversion recovery background suppression preparation. (**c**) The VSASL MBF map at V_C of 15 cm/s is not homogenous and overestimates MBF in the lateral wall, indicated by the red arrow. MBF of the lateral wall was 1.12, 1.34, and 5.64 for FAIR and VSASL at V_C of 15 cm/s and 5 cm/s, respectively. We suspect that at V_C of 5 cm/s, overestimation of MBF in the lateral wall is because of spurious labeling of moving myocardium. Units are in ml/g/min.

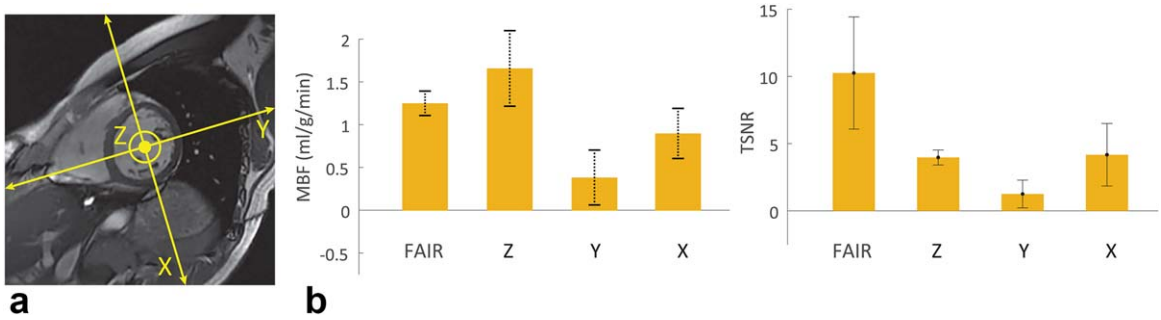

FIG. 5. VSASL sensitivity to the anterior–posterior (X), lateral–septal (Y), and apical–basal (Z) encoding directions. (**a**) Diagram of different encoding directions. (**b**) MBF and TSNR as a function of encoding direction globally averaged across subjects. The radial Y direction severely underestimated MBF and had the lowest TSNR. Performance of X was similar to Z, possibly because of labeling of the left circumflex in X. Detailed analysis of individual segments did not reveal significant differences. Error bars for MBF are in dotted black and represent the average physiological noise across subjects to reflect measurement variability. Error bars for TSNR are in solid black and were calculated as the standard deviation of the TSNR between subjects to reflect intersubject variability.

running in the lateral–septal direction whereas the circumflex runs in the anterior–posterior direction. Nevertheless, we still recommend performing VSASL in the longitudinal Z direction because of its lower intersubject variation as well as the ease of scan prescription.

Measurements from VSASL at V_C of 10 cm/s and FAIR were shown to be statistically equivalent globally using the TOST procedure at a difference of 0.3 ml/g/min ($P = 0.049$). However, differences between VSASL and FAIR were observed with segmental analysis in individual cases (not shown). These differences did not follow a systematic trend. The spatial variance of the difference between FAIR and VSASL (0.32) is close to the squared sum of their respective physiological noise (0.26). This suggests that the observed differences are primarily because of the low TSNR of both VSASL and FAIR at rest.

VSASL had the highest TSNR when performed using a V_C of 10 cm/s in the longitudinal direction. However, it was still 2.8 times lower than the TSNR of FAIR. This is as a result of 50% signal loss from using a saturation pulse as opposed to inversion, as well as 13% signal loss from T_2-weighting during the VS preparation. Despite having lower TSNR, the main advantage of VSASL is its insensitivity to transit delay. Although a high V_C of 10 cm/s reduces transit delay insensitivity, blood within epicardial vessels adjacent to myocardium and within the imaging slice are still labeled. Therefore, transit delay would only depend on the time it takes blood to flow through smaller arterioles to the capillary bed. In contrast, transit delay in whole heart FAIR would also include the time for blood to travel from the aortic root through the epicardial coronary vessels. This study was unable to highlight this advantage though, because VSASL was only compared with single-slice FAIR, where transit delay is only 400 ms (4) in healthy volunteers and has a negligible impact on MBF estimation. A natural follow up to this study would be to perform VSASL in patients with coronary artery disease with collateral circulation (37,38) or in an animal model with slow coronary flow (39).

One drawback of VSASL is its sensitivity to the timing of the label. Rapid variations in heart rate could cause mistriggering and spurious labeling of moving myocardium. A possible solution would be to use an alternate VS pulse with a sharper velocity profile than the sinc-shaped profile of the BIR8 preparation (10). A rectangular velocity profile could be achieved using Shinar-le-Roux (SLR) (12,13). Moreover, the SLR pulse can be designed to achieve inversion rather than saturation to increase the VSASL signal. However, SLR pulses are not adiabatic and would have to be redesigned and tested for off-resonance and B_1 variation found in the heart.

CONCLUSIONS

We have demonstrated the feasibility of using a velocity selective pulse for cardiac ASL and have measured the performance of VSASL under a range of V_C and encoding directions. At the best performing setting using a V_C of 10 cm/s in the longitudinal direction, we found VSASL had 2.8 times lower TSNR than FAIR. We anticipate that TSNR can be improved by using a velocity selective inversion pulse with less sensitivity to myocardial motion.

ACKNOWLEDGMENTS

We thank Eric Wong and Jia Guo for helpful discussions.

REFERENCES

1. Poncelet BP, Koelling TM, Schmidt CJ, Kwong KK, Reese TG, Ledden P, Kantor HL, Brady TJ, Weisskoff RM. Measurement of human myocardial perfusion by double-gated flow alternating inversion recovery EPI. Magn Reson Med 1999;41:510–519.
2. Wacker CM, Bock M, Hartlep AW, Beck G, van Kaick G, Ertl G, Bauer WR, Schad LR. Changes in myocardial oxygenation and perfusion under pharmacological stress with dipyridamole: assessment using T*2 and T1 measurements. Magn Reson Med 1999;41:686–695.
3. Zun Z, Wong EC, Nayak KS. Assessment of myocardial blood flow (MBF) in humans using arterial spin labeling (ASL): feasibility and noise analysis. Magn Reson Med 2009;62:975–983.
4. Wang DJJ, Bi X, Avants BB, Meng T, Zuehlsdorff S, Detre JA. Estimation of perfusion and arterial transit time in myocardium using free-breathing myocardial arterial spin labeling with navigator-echo. Magn Reson Med 2010;64:1289–1295.
5. Zun Z, Varadarajan P, Pai RG, Wong EC, Nayak KS. Arterial spin labeled CMR detects clinically relevant increase in myocardial blood flow with vasodilation. JACC Cardiovasc Imaging 2011;4:1253–1261.

6. Beohar N, Erdogan AK, Lee DC, Sabbah HN, Kern MJ, Teerlink J, Bonow RO, Gheorghiade M. Acute heart failure syndromes and coronary perfusion. J Am Coll Cardiol 2008;52:13–16.
7. Lund GK, Watzinger N, Saeed M, Reddy GP, Yang M, Araoz PA, Curatola D, Bedigian M, Higgins CB. Chronic heart failure: global left ventricular perfusion and coronary flow reserve with velocity-encoded cine MR imaging: initial results. Radiology 2003;227:209–215.
8. Muehling OM, Huber A, Cyran C, Schoenberg SO, Reiser M, Steinbeck G, Nabauer M, Jerosch-Herold M. The delay of contrast arrival in magnetic resonance first-pass perfusion imaging: a novel non-invasive parameter detecting collateral-dependent myocardium. Heart 2007;93:842–847.
9. Qiu D, Straka M, Zun Z, Bammer R, Moseley ME, Zaharchuk G. CBF measurements using multidelay pseudocontinuous and velocity-selective arterial spin labeling in patients with long arterial transit delays: comparison with xenon CT CBF. J Magn Reson Imaging 2012; 36:110–119.
10. Wong EC, Cronin M, Wu WC, Inglis B, Frank LR, Liu TT. Velocity-selective arterial spin labeling. Magn Reson Med 2006;55:1334–1341.
11. Wu WC, Wong EC. Intravascular effect in velocity-selective arterial spin labeling: the choice of inflow time and cutoff velocity. Neuroimage 2006;32:122–128.
12. Shin T, Worters PW, Hu BS, Nishimura DG. Non-contrast-enhanced renal and abdominal MR angiography using velocity-selective inversion preparation. Magn Reson Med 2013;69:1268–1275.
13. Qin Q, Shin T, Schär M, Guo H, Chen H, Qiao Y. Velocity-selective magnetization-prepared non-contrast-enhanced cerebral MR angiography at 3 Tesla: improved immunity to B0/B1 inhomogeneity. Magn Reson Med 2016;75:1232–1241.
14. Gorcsan J III, Gulati VK, Mandarino WA, Katz WE. Color-coded measures of myocardial velocity throughout the cardiac cycle by tissue Doppler imaging to quantify regional left ventricular function. Am Heart J 1996;131:1203–1213.
15. Simpson R, Keegan J, Firmin D. Efficient and reproducible high resolution spiral myocardial phase velocity mapping of the entire cardiac cycle. J Cardiovasc Magn Reson 2013;15:34.
16. Anderson HV, Stokes MJ, Leon M, Abu-Halawa SA, Stuart Y, Kirkeeide RL. Coronary artery flow velocity is related to lumen area and regional left ventricular mass. Circulation 2000;102:48–54.
17. Pereira VFA, De Carvalho Frimm C, Rodrigues ACT, Tsutsui JM, Cúri M, Mady C, Ramires JAF. Coronary flow velocity reserve in hypertensive patients with left ventricular systolic dysfunction. Clin Cardiol 2002;25:95–102.
18. Guo J, Meakin JA, Jezzard P, Wong EC. An optimized design to reduce eddy current sensitivity in velocity-selective arterial spin labeling using symmetric BIR-8 pulses: reduced EC sensitivity in VSASL using symmetric BIR-8 pulses. Magn Reson Med 2015;73: 1085–1094.
19. Meakin JA, Jezzard P. An optimized velocity selective arterial spin labeling module with reduced eddy current sensitivity for improved perfusion quantification. Magn Reson Med 2013;69:832–838.
20. Sung K, Nayak KS. Measurement and characterization of RF nonuniformity over the heart at 3T using body coil transmission. J Magn Reson Imaging 2008;27:643–648.
21. Schär M, Kozerke S, Fischer SE, Boesiger P. Cardiac SSFP imaging at 3 Tesla. Magn Reson Med 2004;51:799–806.
22. Fan Z, Sheehan J, Bi X, Liu X, Carr J, Li D. 3D noncontrast MR angiography of the distal lower extremities using flow-sensitive dephasing (FSD)-prepared balanced SSFP. Magn Reson Med 2009;62:1523–1532.
23. Maleki N, Dai W, Alsop DC. Optimization of background suppression for arterial spin labeling perfusion imaging. MAGMA 2011;25:127–133.
24. Kellman P, McVeigh ER. Image reconstruction in SNR units: a general method for SNR measurement. Magn Reson Med 2005;54:1439–1447.
25. Javed A, Jao TR, Nayak KS. Motion correction facilitates the automation of cardiac ASL perfusion imaging. J Cardiovasc Magn Reson 2015;17(Suppl 1):P51.
26. Cerqueira MD, Weissman NJ, Dilsizian V, Jacobs AK, Kaul S, Laskey WK, Pennell DJ, Rumberger JA, Ryan T, Verani MS. Standardized myocardial segmentation and nomenclature for tomographic imaging of the heart a statement for healthcare professionals from the cardiac imaging committee of the Council on Clinical Cardiology of the American Heart Association. Circulation 2002;105:539–542.
27. Jao T, Zun Z, Varadarajan P, Pai R, Nayak K. Mapping of myocardial ASL perfusion and perfusion reserve data. In Proceedings of the 19th Scientific Sessions of ISMRM, Montreal, Canada, 2011. p. 1339.
28. Buxton RB, Frank LR, Wong EC, Siewert B, Warach S, Edelman RR. A general kinetic model for quantitative perfusion imaging with arterial spin labeling. Magn Reson Med 1998;40:383–396.
29. Zhao JM, Clingman CS, Närväinen MJ, Kauppinen RA, van Zijl PCM. Oxygenation and hematocrit dependence of transverse relaxation rates of blood at 3T. Magn Reson Med 2007;58:592–597.
30. Rahimtoola SH. Hibernating myocardium has reduced blood flow at rest that increases with low-dose dobutamine. Circulation 1996;94: 3055–3061.
31. Chareonthaitawee P, Kaufmann PA, Rimoldi O, Camici PG. Heterogeneity of resting and hyperemic myocardial blood flow in healthy humans. Cardiovasc Res 2001;50:151–161.
32. Hsu LY, Rhoads KL, Holly JE, Kellman P, Aletras AH, Arai AE. Quantitative myocardial perfusion analysis with a dual-bolus contrast-enhanced first-pass MRI technique in humans. J Magn Reson Imaging 2006;23:315–322.
33. Walker E, Nowacki AS. Understanding equivalence and noninferiority testing. J Gen Intern Med 2011;26:192–196.
34. Wacker CM, Fidler F, Dueren C, Hirn S, Jakob PM, Ertl G, Haase A, Bauer WR. Quantitative assessment of myocardial perfusion with a spin-labeling technique: preliminary results in patients with coronary artery disease. J Magn Reson Imaging 2003;18:555–560.
35. Northrup BE, McCommis KS, Zhang H, Ray S, Woodard PK, Gropler RJ, Zheng J. Resting myocardial perfusion quantification with CMR arterial spin labeling at 1.5 T and 3.0 T. J Cardiovasc Magn Reson 2008;10:53.
36. Keith GA, Rodgers CT, Chappell MA, Robson MD. A look-locker acquisition scheme for quantitative myocardial perfusion imaging with FAIR arterial spin labeling in humans at 3 tesla. Magn Reson Med 2017;78:541–549.
37. Sabia PJ, Powers ER, Jayaweera AR, Ragosta M, Kaul S. Functional significance of collateral blood flow in patients with recent acute myocardial infarction. A study using myocardial contrast echocardiography. Circulation 1992;85:2080–2089.
38. Seiler C, Fleisch M, Garachemani A, Meier B. Coronary collateral quantitation in patients with coronary artery disease using intravascular flow velocity or pressure measurements. J Am Coll Cardiol 1998;32:1272–1279.
39. Hu L, Bai Y, Gu Y, Yu D, Peng S, Liu X, Zhang M, Liu T, Hu S. Establishment of an experimental angiographic slow coronary flow model by microsphere embolism in swines. Int J Cardiol 2014;176: 1123–1125.

SUPPORTING INFORMATION

Additional Supporting Information may be found in the online version of this article.

Fig. S1. Representative baseline images from 2 volunteers using snapshot SSFP with imaging parameters TR/TE/FA of 3.2 ms/1.5 ms/500, acquired matrix size of 96×96, GRAPPA (24 ACS, 60 acquired). Myocardial signal was used for quantification rather than arterial blood signal, as formulated in Buxton's original kinetic model, because the blood signal was well approximated by the myocardial signal when using the prescribed imaging parameters. In volunteer A, myocardial signal, SMYO, was 1.72 a.u. and left ventricular blood signal, SLV, was 1.76 a.u., resulting in a 2.3% signal difference. In volunteer B, SMYO was 1.93 a.u. and SLV was 2.21, resulting in a 12.7% signal difference.

Table S1. VSASL sensitivity to velocity cutoff for individual subjects. MBF, PN, and TSNR are shown in MBF $\pm$ PN (TSNR) format. MBF and PN are in units of ml/g/min. VSASL settings that achieved the highest TSNR are bolded. At V_C of 10 or 20 cm/s, TSNR was optimal for all subjects. However, TSNR was 2.8 times lower in VSASL compared to FAIR on average. This is because of signal loss from using a saturation as opposed to inversion along with additional T_2 losses from the VS pulse.

Table S2. VSASL sensitivity to velocity encoding direction for individual subjects. MBF, PN, and TSNR are shown in MBF $\pm$ PN (TSNR) format. MBF and PN are in units of ml/g/min. VSASL settings that achieved the highest TSNR are bolded. TSNR was optimal in the longitudinal Z and radial X direction in all subjects. * = rejected from equivalency test (TOST) between FAIR and VSASL because PN >50% MBF from FAIR.